ChinaXiv合作期刊

Up-conversion Properties of Er^{3+}/Yb^{3+} Co-doped $Li_3Ba_2Gd_3(MoO_4)_8$ Phosphors

SONG Ming-Jun(宋明君)[1];ZHANG Yan(张彦)[2];ZHANG Na-Na(张娜娜)[1];WANG Lin-Tong(王林同)[1];MENG Qin-Guo(孟庆国)[1]

[1]*School of Chemistry and Chemical Engineering, Weifang University, Weifang* 261061, *China*;[2]*School of Materials Science and Engineering, Shanghai Institute of Technology, Shanghai* 200235, *China*

ABSTRACT Er^{3+}/Yb^{3+} co-doped $Li_3Ba_2Gd_3(MoO_4)_8$ phosphors were synthesized by conventional solid state reaction method, and their structure and spectral properties were investigated. The diffuse reflectance spectra showed that the $^4I_{15/2} \rightarrow {}^4I_{11/2}$ transition of Er^{3+} and the $^2F_{7/2} \rightarrow {}^2F_{5/2}$ transition of Yb^{3+} ions were highly overlapped. Under the excitation of 980 nm, three up-conversion (UC) luminescence bands around 530, 555 and 660 nm were observed, corresponding to the $^2H_{11/2} \rightarrow {}^4I_{15/2}$, $^4S_{3/2} \rightarrow {}^4I_{15/2}$ and $^4F_{9/2} \rightarrow {}^4I_{15/2}$ transitions of Er^{3+} ions, respectively. The effects of the concentration and pumping power on the UC intensities of $Li_3Ba_2Gd_3(MoO_4)_8:Er^{3+}/Yb^{3+}$ phosphors were investigated, and the possible UC mechanism was proposed based on the results.

Keywords: up-conversion; molybdate compounds; phosphors, energy transfer;

DOI: 10.14102/j.cnki.0254-5861.2011-1753

chinaXiv:201711.00128v1

1 INTRODUCTION

As we know, up-conversion (UC) process has provided a possibility to convert infrared pumping source into visible radiation, which has potential applications in the fields of solid-state lasers, multicolor displays, solar cells, temperature sensing, *etc.*[1-5]. As a consequence, with the rapid development of diode lasers in the infrared region over the past decades, considerable attention has been devoted to infrared-to-visible UC luminescence materials. Among the rare earth ions, Er^{3+} may be the most frequently investigated activator for UC process, since its complicated energy level scheme with many meta-stable excited states gives rise to multi-step energy transfer and excited-state absorption process. However, the main disadvantage of Er^{3+} should be its low absorption cross-section in the laser diodes emission range (0.8～1.5 mm), which greatly

ChinaXiv合作期刊

limits pump efficiency. One possible solution is adding a second ion as sensitizer and Yb^{3+} is often used for this role because of its large absorption cross-section at 980 nm. Furthermore, the energy gap of $^2F_{7/2}\rightarrow{}^2F_{5/2}$ levels of Yb^{3+} ion is very close to that of $^4I_{15/2}\rightarrow{}^4I_{11/2}$ and $^4I_{11/2}\rightarrow{}^4F_{7/2}$ levels of Er^{3+} ion, which allows an efficient energy transfer from Yb^{3+} to Er^{3+} by resonance interaction.

Furthermore, the properties of the host materials, including phonon energy, mechanical robustness and thermal stability, also exert an important effect on the performance of UC. To achieve a high efficiency of UC process, one of the most important requirements is that the host materials should have low phonon energy. Therefore, the current choice of potential host materials for UC mainly concentrates on chlorides, fluorides, and sulfur oxides. These materials are characterized by low phonon energy, which give rise to high UC efficiency[6-8], but their applications are restricted by their unstable chemical nature and poor mechanical robustness[9]. Furthermore, fluorides and sulfur oxides inevitably cause environmental pollution because of the high content of fluorine and sulfur. In recent years, the molybdate based materials have been intensively studied as promising host for solid state lasers and luminescent phosphors owing to their excellent properties, such as excellent chemical stability, moderate synthesis conditions and pollution-free features. In addition, since they also have relatively low lattice phonon energy, many molybdate compounds were also reported as UC host, like $CaMoO_4:Er^{3+}/Yb^{3+}$[1], $ALn(MoO_4)_2:Er^{3+}/Yb^{3+}$ (A = Li, Na and K; Ln = La, Gd and Y)[9], $BaGd_2(MoO_4)_4:Er^{3+}/Yb^{3+}$[10], $Gd_2(MoO)_3:Er^{3+}/Yb^{3+}$[11], and so forth.

The triple molybdate compounds $Li_3Ba_2Re_3(MoO_4)_8$ (Re = La～Lu, Y) belong to the monoclinic system with *C*2/*c* group. In the past, the interest in these compounds mainly concentrated on the bulk crystals to take advantages of their laser properties because of their wonderful spectral properties and simple growth techniques. Notably, efficient laser performance has already been achieved with $Yb^{3+}:Li_3Ba_2Gd_3(MoO_4)_8$[12] and $Tm^{3+}:Li_3Ba_2Lu_3(MoO_4)_8$ crystals[13]. In recent papers, $Li_3Ba_2Re_3(MoO_4)_8$ was further investigated as potential hosts for rare earth ions to develop luminescent materials, and Eu^{3+}, Tb^{3+} and Dy^{3+}-doped $Li_3Ba_2Re_3(MoO_4)_8$ phosphors have been reported for white-light emitting applications[14-16]. However, to the best of our knowledge, these compounds have never been investigated as UC host. So, in the present paper, Er^{3+}/Yb^{3+} co-doped $Li_3Ba_2Gd_3(MoO_4)_8$ was synthesized by solid state reaction method and their UC properties were recorded under the excitation of 980 nm. Moreover, the effect of Er^{3+}/Yb^{3+} concentration and pump power on the UC emission, as well as the possible UC mechanism was also presented.

2 EXPERIMENTAL

chinaXiv:201711.00128v1

ChinaXiv合作期刊

The $Li_3Ba_2Gd_3(MoO_4)_8:Er^{3+}/Yb^{3+}$ phosphors were synthesized by means of solid state reaction method with raw materials of Li_2CO_3 (A.R.), $BaCO_3$ (A.R.), Gd_2O_3 (99.999%), Er_2O_3 (99.99%), Yb_2O_3 (99.99%) and MoO_3 (A.R.). Firstly, a stoichiometric mixture of the raw materials was ball-milled for 10 h using planetary milling with zirconia ball and alcohol media. Then, the dried powders were placed into alumina crucibles and calcined at 900 ℃ for 6 h under air atmosphere. After that, the synthesized samples were grounded into fine powders in an agate mortar for measurement.

The structures of $Li_3Ba_2Gd_3(MoO_4)_8:Er^{3+}/Yb^{3+}$ phosphors were analyzed by X-ray power diffraction (D8 Advance diffractometer, Bruker Corporation, Germany) with a Cu$K\alpha$ radiation (λ = 1.54056 Å, 40 kV, 30 mA). The diffuse reflection spectra were measured using a Shimadzu UV-vis-NIR spectrophotometer (UV-3600). The UC luminescence spectra and luminescence decay curves were recorded using an Edinburgh Instruments FLS980 spectrophotometer equipped with an external power-controllable 980 nm semiconductor laser as excitation source. All the measurements were carried out at room temperature.

3 RESULTS AND DISCUSSION

The X-ray diffraction (XRD) patterns of $Li_3Ba_2Gd_3(MoO_4)_8:Er^{3+}/Yb^{3+}$ phosphors are shown in Fig. 1 and compared with that of pure $Li_3Ba_2Gd_3(MoO_4)_8$. As we can see, all the diffraction peaks of the synthesized samples are consistent with those of pure $Li_3Ba_2Gd_3(MoO_4)_8$ on the powder standard card and no additional diffraction peaks were observed, indicating that all the Er^{3+} and Yb^{3+} ions have been completely doped into the host matrix and substitute for the Gd^{3+} ions. However, as shown in Fig. 1(b), the main diffraction peaks of the samples gradually shift to higher 2θ angles with the increasing concentration of Yb^{3+} ions owing to the smaller radius of Yb^{3+} ions compared to that of Gd^{3+} ions.

To investigate the energy level structures of Er^{3+} and Yb^{3+} ions in the $Li_3Ba_2Gd_3(MoO_4)_8$ host, the absorption spectra of $Li_3Ba_2Gd_3(MoO_4)_8:Er^{3+}/Yb^{3+}$ phosphors were recorded. Fig. 2 shows the diffuse reflection spectra of $Li_3Ba_2Gd_3(MoO_4)_8$:20%Yb^{3+}, $Li_3Ba_2Gd_3(MoO_4)_8$:2%Er^{3+} and $Li_3Ba_2Gd_3(MoO_4)_8$:2%Er^{3+}/20%Yb^{3+} phosphors. For all the samples, a broad and smooth absorption band around 280 nm can be observed, which belongs to the charge transfer transition of O → Mo. Besides, six eminent absorption bands around 380, 485, 520, 655, 800 and 975 nm can be also observed with the $Li_3Ba_2Gd_3(MoO_4)_8$:2%Er^{3+} and $Li_3Ba_2Gd_3(MoO_4)_8$:2%Er^{3+}/20%Yb^{3+} phosphors. The former five absorption

chinaXiv:201711.00128v1

ChinaXiv合作期刊

bands for the two samples are very similar and can be ascribed to the intrinsic transitions of Er^{3+} ions from the ground state of $^4I_{15/2}$ to the excited states of $^4G_{11/2}$, $^4F_{7/2}$, $^2H_{11/2}$, $^4F_{9/2}$ and $^4I_{9/2}$, respectively. However, it should be noted that the absorption band around 975 nm of $Li_3Ba_2Gd_3(MoO_4)_8$:2%Er^{3+} is much weaker than that of $Li_3Ba_2Gd_3(MoO_4)_8$:2%Er^{3+}/20%Yb^{3+}. For $Li_3Ba_2Gd_3(MoO_4)_8$:2%Er^{3+}, the absorption band peak at 974 nm comes from the $^4I_{15/2}\rightarrow{}^4I_{11/2}$ transition of Er^{3+} ions, while the one for $Li_3Ba_2Gd_3(MoO_4)_8$:2%Er^{3+}/20%Yb^{3+} at 968 nm should be the superposition of the $^2F_{7/2}\rightarrow{}^2F_{5/2}$ transition of Yb^{3+} ions and the $^4I_{15/2}\rightarrow{}^4I_{11/2}$ transition of Er^{3+} ions. As for the sample of $Li_3Ba_2Gd_3(MoO_4)_8$:20%Yb^{3+}, only an intensive band is found around 975 nm, which arises from the $^2F_{7/2}\rightarrow{}^2F_{5/2}$ transition of Yb^{3+} ions. According to Fig. 2, it can be concluded that the energy transfer process between Yb^{3+} and Er^{3+} ions in $Li_3Ba_2Gd_3(MoO_4)_8$ should be very effective because of the significant overlaps between the $^4I_{15/2}\rightarrow{}^4I_{11/2}$ transition of Er^{3+} and the $^2F_{7/2}\rightarrow{}^2F_{5/2}$ transition of Yb^{3+} ions.

Under the excitation of 980 nm, the UC luminescence spectra of $Li_3Ba_2Gd_3(MoO_4)_8$:2%Er^{3+}/$x$$Yb^{3+}$ (x = 8%, 12%, 16%, 20%, 24%, 28%) phosphors in the wavelength range of 500～700 nm were recorded, as shown in Fig. 3. The UC luminescence spectra of all the recorded samples display similar profiles consisting of three emission bands around 530, 555, and 660 nm. The green emission bands at 530 and 555 nm can be ascribed to the $^2H_{11/2}\rightarrow{}^4I_{15/2}$ and $^4S_{3/2}\rightarrow{}^4I_{15/2}$ transitions of Er^{3+} ions, respectively. The multi-peaks of the two green bands should be caused by crystal-field stark splitting. The red emission band at 660 nm can be ascribed to the $^4F_{9/2}\rightarrow{}^4I_{15/2}$ transition of Er^{3+} ions. In our previous research, a tiny emission band at 490 nm deriving from the $^4F_{7/2}\rightarrow{}^4I_{15/2}$ transition of Er^{3+} ions was also observed with Er^{3+}:$Li_3Ba_2Gd_3(MoO_4)_8$ single crystals under 980 nm excitation[17]. In the present research, however, this emission band is not observed. The main reason may be that the polycrystalline $Li_3Ba_2Gd_3(MoO_4)_8$ possesses much more defects than single-crystal $Li_3Ba_2Gd_3(MoO_4)_8$, which act as nonradiative recombination centers and significantly depopulate of $^4F_{7/2}$ state. The inset of Fig. 3 shows the integrated intensities of green and red emission bands with respect to the Yb^{3+} concentration. As we can see that with increasing the Yb^{3+} concentration, both the green and red emission intensities increase obviously, suggesting an efficient energy transfer of $Yb^{3+}\rightarrow Er^{3+}$. However, when the Yb^{3+} concentration is beyond 20 mol%, both the green and red emission intensities decrease due to the concentration quenching effect. The concentration quenching effect is mainly caused by energy transfer between neighboring Er^{3+} and Yb^{3+} ions. With increasing the Er^{3+} and Yb^{3+} concentrations, the distance between Er^{3+} and Yb^{3+} ions gets shorter, and meanwhile the non-radiative energy transfer becomes more intensive[9]. As a result, the emission intensities of Er^{3+} ions decrease.

chinaXiv:201711.00128v1

ChinaXiv合作期刊

In order to understand the UC mechanism of $Li_3Ba_2Gd_3(MoO_4)_8:Er^{3+}/Yb^{3+}$, the UC luminescence spectra of $Li_3Ba_2Gd_3(MoO_4)_8$:2%Er^{3+}/20%Yb^{3+} phosphors were measured as a function of different pumping powers (Fig. 4). As we can see that there is hardly any difference among the profiles of the UC luminescence spectra, but the emission intensities increase with the increasing pumping powers. The relation between the UC luminescence intensity and the pumping powers can be described by the following equation[18]:

$$I_{em} \propto P_{pump}^{n} \tag{1}$$

where I_{em} is the UC luminescence intensity, P_{pump} is the pumping powers and n represents the number of photons involved in the UC process. Generally, the above equation is written as:

$$\ln I_{em} = n \ln P_{pump} \tag{2}$$

The plots of $\ln I_{em}$ for the three emission bands versus $\ln P_{pump}$ yield straight lines, as shown in the inset of Fig. 4. By linear fitting, the slope values n were obtained to be 2.03, 1.85, 1.80 for 530, 555 and 660 nm emission respectively, which are close to 2. So, we can conclude that two photons are involved for the UC process in the system of $Li_3Ba_2Gd_3(MoO_4)_8:Er^{3+}/Yb^{3+}$.

The UC mechanism in Er^{3+}/Yb^{3+} co-doped systems has been extensively investigated in many literatures[1-6]. It can be described by the energy level diagram sketched in Fig. 5. Under the excitation of 980 nm, the Yb^{3+} ions can be excited to the excited-state of $^2F_{5/2}$. Meanwhile, the Er^{3+} can also be exited to its excited-state of $^4I_{11/2}$ through ground state absorption (GSA) process and energy transfer (ET) process:

GSA: $^4I_{15/2}$ (Er^{3+}) + a photon (980 nm) → $^4I_{11/2}$

ET: $^4I_{15/2}$ (Er^{3+}) + $^2F_{5/2}$ (Yb^{3+}) → $^4I_{11/2}$ (Er^{3+}) + $^2F_{7/2}$ (Yb^{3+})

Since the lifetime of $^4I_{11/2}$ state of Er^{3+} is very long[19], it is expected that the population of this excited state can be further excited to the upper state of $^4F_{7/2}$ through excited state absorption (ESA) process and energy transfer (ET) process:

ESA: $^4I_{11/2}$ (Er^{3+}) + a photon (980 nm) → $^4I_{7/2}$

ET: $^4I_{11/2}$ (Er^{3+}) + $^2F_{5/2}$ (Yb^{3+}) → $^4I_{7/2}$ (Er^{3+}) + $^2F_{7/2}$ (Yb^{3+})

Some of the populations of the $^4F_{7/2}$ state relax non-radiatively to the $^2H_{11/2}$ and $^4S_{3/2}$ states, giving rise to the green emissions of 530 and 555 nm, respectively. At the same time, some of the populations of the $^4F_{7/2}$ state relax non-radiatively to the $^4F_{9/2}$ state, from which the red emission of 660 nm is observed.

The decay curves of the $^2H_{11/2}$→$^4I_{15/2}$ (530 nm), $^4S_{3/2}$→$^4I_{15/2}$ (555nm) and $^4F_{9/2}$→$^4I_{15/2}$ (660nm) transitions of Er^{3+} ions in $Li_3Ba_2Gd_3(MoO_4)_8$:2%Er^{3+} and $Li_3Ba_2Gd_3(MoO_4)_8$:2%Er^{3+}/20%Yb^{3+} samples were

chinaXiv:201711.00128v1

ChinaXiv合作期刊

measured under 980 nm excitation. As shown in Fig. 6, the decay curves of the three transitions in $Li_3Ba_2Gd_3(MoO_4)_8$:2%Er^{3+} exhibit a typical single exponential behavior, and the lifetimes were calculated to be 21.6, 20.7 and 22.4 μs by linear fitting. However, the decay curves of $Li_3Ba_2Gd_3(MoO_4)_8$:2%Er^{3+}/20%Yb^{3+} sample are not single exponential and can be fitted with a second-order exponential model:

$$I(t) = A_1 \exp(-t/t_1) + A_2 \exp(-t/t_2) \quad (3)$$

where I is the UC luminescence intensity, A_1 and A_2 are constants, t_1 and t_2 are the lifetimes for the exponential components. The values of A_1, A_2, t_1 and t_2 are presented in Table 1. The mean lifetimes for the three transitions in $Li_3Ba_2Gd_3(MoO_4)_8$:2%Er^{3+}/20%Yb^{3+} sample can be calculated by the following equation[20]:

$$\tau_{mean} = (A_1 t_1^2 + A_2 t_1^2)/(A_1 t_1 + A_2 t_2) \quad (4)$$

The mean lifetimes of $Li_3Ba_2Gd_3(MoO_4)_8$:2%Er^{3+}/20%Yb^{3+} are also listed in Table 1. As we can see that the lifetimes in $Li_3Ba_2Gd_3(MoO_4)_8$:2%Er^{3+}/20%Yb^{3+} sample are much larger than those in $Li_3Ba_2Gd_3(MoO_4)_8$:2%Er^{3+} sample, which should be caused by energy transfer from Yb^{3+} to Er^{3+} ions.

4 CONCLUSION

A serious of $Li_3Ba_2Gd_3(MoO_4)_8$:Er^{3+}/Yb^{3+} phosphors were synthesized by conventional solid state reaction method and their structures were confirmed by X-ray diffraction method. Under the excitation of 980 nm, the samples exhibited a weak red UC emission at 660 nm and two strong green UC emissions at 530 and 555 nm. With a fixed Er^{3+} concentration of 2 mol%, the effects of Yb^{3+} concentrations on the UC luminescence properties were investigated and the optimum concentration of Yb^{3+} is determined to be 20 mol%. The relations between UC emission intensities and pumping powers were investigated and the result revealed that a two photons process was responsible for all the three observed UC emissions. The lifetimes for both the $Li_3Ba_2Gd_3(MoO_4)_8$:2%Er^{3+} and $Li_3Ba_2Gd_3(MoO_4)_8$:2%Er^{3+}/20%Yb^{3+} samples were measured and the results showed that the introduction of Yb^{3+} had greatly enhanced the lifetimes of Er^{3+} ions.

Table 1. Lifetimes of the $^2H_{11/2}$, $^4S_{3/2}$ and $^4F_{9/2}$ States of Er^{3+} Ions for $Li_3Ba_2Gd_3(MoO_4)_8$:2%Er^{3+} and $Li_3Ba_2Gd_3(MoO_4)_8$:2%Er^{3+}/20%Yb^{3+} Samples

chinaXiv:201711.00128v1

ChinaXiv合作期刊

Samples	Transitions	Lifetime (μs)
$Li_3Ba_2Gd_3(MoO_4)_8$:2%Er^{3+}	$^2H_{11/2}\rightarrow{}^4I_{15/2}$	21.6
	$^4S_{3/2}\rightarrow{}^4I_{15/2}$	20.7
	$^4F_{9/2}\rightarrow{}^4I_{15/2}$	22.4
$Li_3Ba_2Gd_3(MoO_4)_8$:2%Er^{3+}/20%Yb^{3+}	$^2H_{11/2}\rightarrow{}^4I_{15/2}$	A_1=1211.6, t_1=117.8
		A_2=11.2, t_2=537.2
		τ_{mean} = 134.7
	$^4S_{3/2}\rightarrow{}^4I_{15/2}$	A_1=510.6, t_1=162.7
		A_2=1025.3, t_2=66.4
		τ_{mean} =119.3
	$^4F_{9/2}\rightarrow{}^4I_{15/2}$	A_1=874.9, t_1=83.8
		A_2=311.1, t_2=238.4
		τ_{mean} =161.5

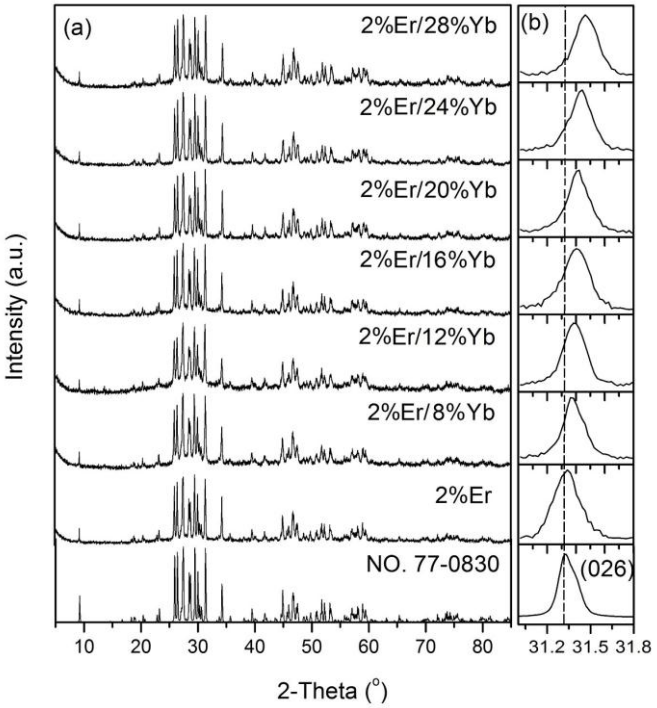

Fig. 1. XRD patterns of $Li_3Ba_2Gd_3(MoO_4)_8$:2%Er^{3+}/xYb^{3+} with different Yb^{3+} concentrations

chinaXiv:201711.00128v1

ChinaXiv合作期刊

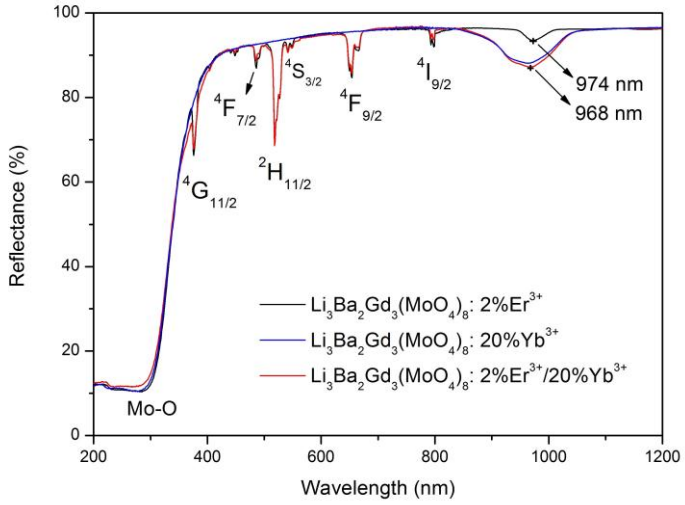

Fig. 2. Diffraction reflectance spectra of $Li_3Ba_2Gd_3(MoO_4)_8$:2%Er^{3+}, $Li_3Ba_2Gd_3(MoO_4)_8$:20%Yb^{3+} and $Li_3Ba_2Gd_3(MoO_4)_8$:2%Er^{3+}/20%Yb^{3+}

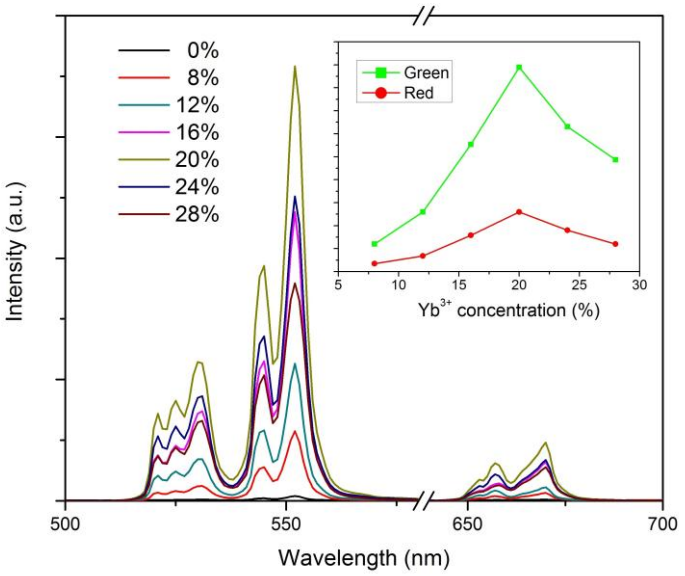

Fig. 3. UC luminescence spectra of $Li_3Ba_2Gd_3(MoO_4)_8$:2%Er^{3+}/xYb^{3+} with different Yb^{3+} concentrations. The inset shows the dependence of green and red UC emission intensity on the Yb^{3+} concentration

chinaXiv:201711.00128v1

ChinaXiv合作期刊

chinaXiv:201711.00128v1

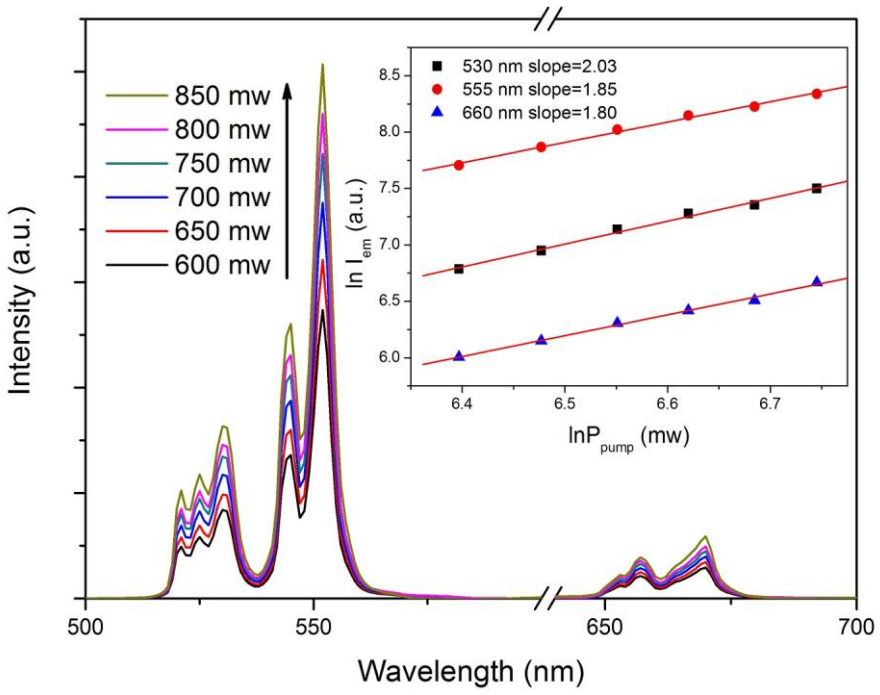

Fig. 4. UC luminescence spectra of $Li_3Ba_2Gd_3(MoO_4)_8$:2%Er^{3+}/20%Yb^{3+} with different pumping powers. The inset shows the power dependence of UC emission intensity at 530, 555 and 660 nm

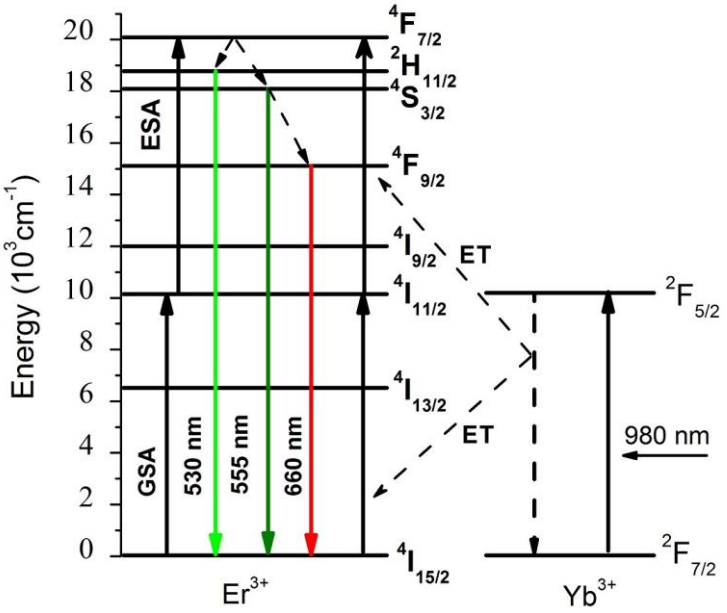

Fig. 5. Energy level scheme of Er^{3+} and Yb^{3+} in $Li_3Ba_2Gd_3(MoO_4)_8$ and the possible UC mechanisms under 980 nm excitation

ChinaXiv合作期刊

chinaXiv:201711.00128v1

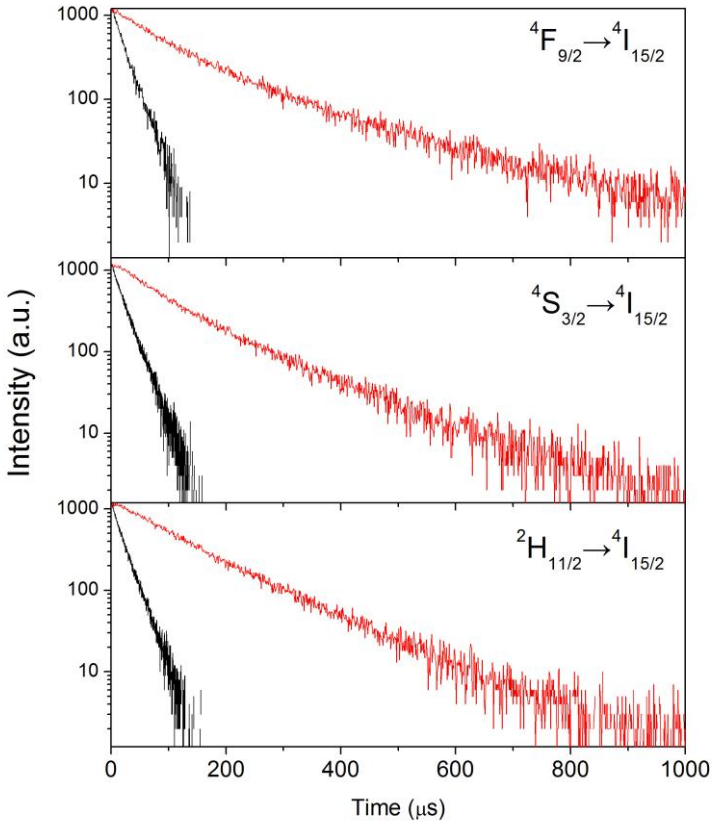

Fig. 6. Decay curves of $^2H_{11/2}$, $^4S_{3/2}$ and $^4F_{9/2}$ states for $Li_3Ba_2Gd_3(MoO_4)_8$:2%Er^{3+} (black) and $Li_3Ba_2Gd_3(MoO_4)_8$:2%Er^{3+}/20%Yb^{3+} (red) samples

REFERENCES

(1) Chuang, J. H.; Ryu, J. H.; Eun, J. W.; Lee, J. H.; Lee, S. Y.; Heo, T. H.; Choi, B. G.; Shim, K. B. Green upconversion luminescence from poly-crystalline Yb^{3+}, Er^{3+} co-doped $CaMoO_4$. *J. Alloys Compd*. **2012**, 522, 30–34.

(2) Mei, L. F.; Xie, J.; Liao, L. B.; Guan, M.; Liu, H. K. Tunable upconversion luminescence and energy transfer process in $BaLa_2ZnO_5$:Er^{3+}/Yb^{3+} phosphors. *Adv. Mter. Sci. Eng*. **2015**, 2015, 1–5.

(3) Das, S.; Reddy, A. A.; Babu, S. S.; Prakash, G. V. Tunable visible upconversion emission in Er^{3+}/Yb^{3+}-codoped $KCaBO_3$ phosphors by introducing Ho^{3+} ions. *Mater. Lett*. **2014**, 120, 232–235.

(4) Guan, M.; Zheng, H.; Mei, L. F.; Molokeev, M. S.; Xie, J.; Yang, T.; Wu, X. W.; Huang, S. F.; Huang, Z. H. Preparation, structure, and up-conversion luminescence of Yb^{3+}/Er^{3+} codoped $SrIn_2O_4$ phosphors. *J. Am. Ceram. Soc*. **2015**, 98, 1182–1187.

(5) Wei, X.; Zhang, Z. G.; Cao, W. W. Excellent optical thermometry based on short-wavelength upconversion emissions in Er^{3+}/Yb^{3+} codoped $CaWO_4$. *Opt. Lett*. **2012**, 37, 4865–4867.

(6) Pokhrel, M.; Gangadharan, A.; Sardar, D. K. High upconversion quantum yield at low pump threshold in Er^{3+}/Yb^{3+} doped La_2O_2S phosphor. *Mater. Lett*. **2013**, 99, 86–89.

(7) Li, C. X.; Lin, J. Rare earth fluoride nano-/microcrystals: synthesis, surface modification and application. *J. Mater. Chem*. **2010**, 20, 6831–3847.

(8) Ding, M. Y.; Chen, D. Q.; Chen, T. J.; Lu, C. H.; Ni, Y. R.; Xu, Z. Z. Hydrothermal synthesis and upconversion luminescence properties of BaFCl:Yb^{3+}/Er^{3+} microhseets. *Mater. Lett*. **2014**, 128, 101–104.

(9) Li, T.; Guo, C. F.; Wu, Y. R.; Li, L.; Jeong, J. H. Green upconversion luminescence in Yb^{3+}/Er^{3+} co-doped $ALn(MoO_4)_2$ (A = Li, Na and K; Ln = La, Gd and Y). *J. Alloys Compd*. **2012**, 540, 107–112.

(10) Sun, J. Y.; Lan, Y. J.; Xia, Z. G.; Du, H. Y. Sol-gel synthesis and green upconversion luminescence in $BaGd_2(MoO_4)_4$:Yb^{3+}, Er^{3+} phosphors. *Opt.*

ChinaXiv合作期刊

Mater. **2011**, 33, 576–581.

(11) Lu, H. Y.; Gao, Y. C.; Hao, H. Y.; Shi, G.; Li, D. Y.; Song, Y. L.; Wang, Y. X.; Zhang, X. R. Judd-Ofelt analysis and temperature dependent upconversion luminescence of Er^{3+}/Yb^{3+} odoped $Gd_2(MoO_4)_3$ phosphor. *J. Lumin.* **2017**, 186, 34–39.

(12) Garcá-Cortés, A.; Zaldo, C.; Cascales, C.; Mateos, X.; Petrov, V. Laser operation of Yb^{3+} in disordered $Li_{0.75}Gd_{0.75}Ba_{0.5}(MoO_4)_2$ crystal with small quantum defect. *Opt. Express* **2007**, 15, 18162–18167.

(13) Rico, M.; Han, X. M.; Cascales, C.; Esteban-Betegón, F.; Zaldo, C. Efficient mid-infrared laser operation of $Li_3Lu_{3-x}Tm_xBa_2(MoO_4)_8$ disordered crystal. *Opt. Express* **2011**, 19, 7640–7645.

(14) Guo, C. F.; Gao, F.; Liang, L. F.; Choi, B. C.; Jeong, J. H. Synthesis, characterization and luminescent properties of novel red emitting phosphor $Li_3Ba_2Ln_3(MoO_4)_8:Eu^{3+}$ (Ln = La, Gd and Y) for white light-emitting diodes. *J. Alloys Compd*. **2009**, 479, 607–612.

(15) Mo, F. W.; Chen, P. C.; Guan, A. X.; Zhang, X. G.; Xu, C. Y.; Zhou, L. Y. Synthesis and luminescence enhancement of $Li_3Ba_2Gd_{2.95-y}Eu_{0.05}M_y(MoO_4)_8$ (M = Bi^{3+}, Sm^{3+}) phosphors based on energy transfer. *Ceram. Int*. **2015**, 41, 707–713.

(16) Shang, M. M.; Li, G. G.; Kang, X. J.; Yang, D. M.; Lin, J. Synthesis and luminescent properties of $Li_3Ba_2Y_3(MoO_4)_8:Ln^{3+}$ (Ln = Eu, Tb, Dy) phosphors for UV-LEDs. *J. Electrochem. Soc*. **2011**, 158, H565–H571.

(17) Song, M. J.; Wang, L. T.; Zhao, M. L.; Zhang, L. Z.; Wang, G. F. Optical spectroscopy, 1.5 μm emission and up-conversion properties of Er^{3+}-doped $Li_3Ba_2Gd_3(MoO_4)_8$ crystal. *J. Lumin*. **2011**, 131, 1571–1576.

(18) Chamarro, M. A.; Cases, R. Infrared to visible upconversion of Er^{3+} ions in Yb^{3+} doped fluorohafnate glasses. *J. Lumin*. **1990**, 46, 59–65.

(19) Capobianco, J. A.; Kabro, P.; Ermeneux, F. S.; Moncorgé, R.; Bettinelli, M.; Cavalli, E. Optical spectroscopy, fluorescence dynamics and crystal-field analysis of Er^{3+} in YVO_4. *Chem. Phys*. **1997**, 214, 329–340.

(20) Xia, Z. G.; Li, J.; Luo, Y.; Liao, L. B. Comparative investigation of green and red upconversion luminescence in Er^{3+} doped and Yb^{3+}/Er^{3+} codoped LaOCl. *J. Am. Ceram. Soc*. **2012**, 95, 3229–3234.

chinaXiv:201711.00128v1

Up-conversion Properties of Er^{3+}/Yb^{3+} Co-doped $Li_3Ba_2Gd_3(MoO_4)_8$ Phosphors

SONG Ming-Jun(宋明君)　ZHANG Yan(张彦)　ZHANG Na-Na(张娜娜)

WANG Lin-Tong(王林同)　MENG Qin-Guo(孟庆国)

$Li_3Ba_2Gd_3(MoO_4)_8:Er^{3+}/Yb^{3+}$ phosphors were synthesized by conventional solid state reaction method, and their structures and spectral properties were investigated. Under 980 nm excitation, three up-conversion (UC) luminescence bands around 530, 555 and 660 nm were observed, corresponding to the $^2H_{11/2}\rightarrow{}^4I_{15/2}$, $^4S_{3/2}\rightarrow{}^4I_{15/2}$ and $^4F_{9/2}\rightarrow{}^4I_{15/2}$ transitions of Er^{3+} ions, respectively. The dependence of the UC luminescence properties on the concentration of Yb^{3+} ions was investigated and the optimum doping concentration was determined. The relations between UC emission intensities and pumping powers were investigated and a two photons UC mechanism was proposed to explain the observed UC emissions.

ChinaXiv合作期刊

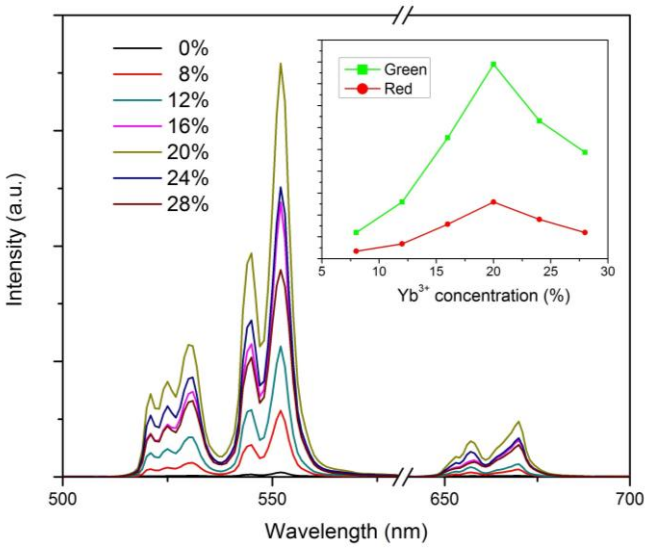

chinaXiv:201711.00128v1